International Journal of Computer Trends and Technology
ISSN: 2231 – 2803 / https://doi.org/10.14445/22312803/IJCTT-V69I7P108

Volume 69 Issue 7, 52-57, July 2021

Original Article

Detection of Mesoscale Eddies using Structural Statistical Feature

Baomin Shao[1], Hongyun Jia[2]

[1]*School of Computer Science and Technology, Shandong, University of Technology, China.*

Received Date: 07 June 2021
Revised Date: 10 July 2021
Accepted Date: 20 July 2021

Abstract *- Because of the size and the increasing quantity of remote sensing marine images, tools are needed for computer-aided research. Automated eddy detection methods are fundamental tools to study mesoscale eddies from the large datasets derived from satellite images. In this work, mesoscale ocean eddies are characterized by currents that flow in a roughly circular motion around the center of the eddy, the sense of rotation of these currents may either be cyclonic or anticyclonic, and a new algorithm is presented to detect eddy centers based on a supervised learning method using support vector machines. A structural statistical feature (SSF) kernel function is introduced in order to favor the distinction between eddy centers and other points. The method learns a generic model for mesoscale eddy by using the SSF of training examples. The algorithm has been applied to over 24 years of AVISO MSLA data derived from current sea data in the global area.*

Keywords *- Eddy detection, Kernel methods, SVM, MSLA, Sea current.*

I. INTRODUCTION

Mesoscale eddies are common in the ocean. They are between about 10 and 500 km in diameter, and persist for periods of days to months, and are characterized by currents that flow in a roughly circular motion around the center of the eddy, the sense of rotation of these currents may either be cyclonic or anticyclonic. Mesoscale eddies are ubiquitous features in the ocean [1-5]. For oceanic mesoscale eddies are usually made of water masses that are different from those outsides of the eddy. The water within an eddy usually has different temperature and salinity characteristics to the water outside of the eddy. Because eddies may have a vigorous circulation associated with them, they are of concern to naval and commercial operations at sea. Further, eddies transport anomalously warm or cold water as they move. They have an important influence on heat transport as well as ocean circulation in certain parts of the ocean[4, 6]. They also have effects on biological productivity, upper ocean ecology, biogeochemistry, and fish larvae transportation[7-11]. In the past few years, several studies have focused on the statistical analysis of mesoscale eddy activity within specific regions through the analysis of satellite measurements or results from numerical models [12,13]. So it is important to develop and implement an algorithm for automatic identification and to track mesoscale eddies to advance research in this area. The aim of this paper is to present a new supervised eddy detection method using 24 years of sea level anomaly (MSLA) data to quantitatively investigate the mesoscale activity and examine its Spatio-temporal variability.

The rest of this paper is organized as follows. Section 2 describes the background of current sea derivation and existing eddy detection methods. The proposed supervised eddy center detection algorithm and the method to label eddies are presented in Section 3. Section 4 gives out the experiment results and comparison with other methods. Some statistical analyses of detected eddies are also described in this section. Finally, Section 5 presents the conclusion.

II. BACKGROUND

A. Sea Current Derivation

The algorithm was developed to detect eddy from a current sea field derived from the MSLA field. The MSLA dataset analyzed here is the 24.5 years (October 1992–March 2017) of the 1/4° latitude by 1/4° longitude global gridded version of the SSH fields in the AVISO Reference Series. Sea surface velocity can be calculated using the geostrophic relation:

$$u = -g/f \cdot \partial h/\partial y \qquad (1)$$

$$v = -g/f \cdot \partial h/\partial x$$

Where u v are the surface velocity(positive eastward and positive northward), g is the gravitational acceleration, and $f = 2\Omega\sin\theta$ ($\Omega = 7.29\times10^{-5} s^{-1}$, θ is the latitude) is the Coriolis parameter, x, y is the distance on two directions, and h is the MSLA? To generate a continuous estimate of u and v across the equator, a Gaussian

adjustment [14] is adopted to calculate the sea current near the equator ($\pm 5^{o}$ Lat).

B. Eddy detection

Existing automatic eddy detection methods mainly fall into two categories, and one is based on the distribution of physical parameters usually computed from velocity derivatives; the other is derived from the geometric characteristic of velocity streamlines around minima or maxima of MSLA[15].

One of the most widely used physical parameters based eddy detection algorithm is developed [16], based on the Okubo-Weiss parameter [17] that indexes the relative importance of strain and vorticity in the flow as

$$W = s_s^{\ 2} + s_n^{\ 2} - \omega^2 \tag{2}$$

where s_s , s_n and ω are the shearing deformation rate, the straining deformation rate, and the vorticity. Since the velocity field within a vortex is dominated by rotation, ocean eddies are generally characterized by negative values W . For this reason, a value can be set as the threshold to identify an eddy. Although this method is often used to extract eddies from MSLA data, some studies have shown limitations of the method. For example, it needs to specify a threshold value from which eddies are defined, but the value has to be adjusted according to the varying eddy location and other properties, and during the computation of the method, it will amplify the noise of the MSLA field. The problem is even more complicated at low latitudes.

The second type of eddy identification technique is based on the geometric characteristics of the sea current. The winding-angle method detects closed streamlines via measuring cumulative changes in streamline direction, and a streamline is associated with an eddy if its winding-angle is higher than 2π . This method has a higher chance of successfully detecting mesoscale eddies. However, it comes at a higher computational cost. Francesco Nencioli [18] presented an eddy detection algorithm based on four geometric constraints, which include: velocity change tendency along east-west and north-south section, local velocity minimum point, and a current sea direction changing the rule. A limitation of this method is it needs two parameters that have to be carefully selected in accordance with data resolution.

III. DETECTION OF EDDY CENTER

A. Support Vector Machine

This section will describe the principle of SVM in a linear separable case. SVMs represented an approximate implementation of the structural risk minimization(SRM) principle and were first introduced by Vapnik [19] to solve pattern recognition and regression estimation problems. Given a set of training examples $(x_i, y_i)_{1\le i\le N}$ $x_i \in R^d$, d is the dimension of the input space $y_i \in \{-1,1\}$ is the class label which x_i belongs to. The aim is to find a hyperplane that divides the set of examples such that all the points with the same label are on the same side of the hyperplane. The general form of linear classification function is $g(x) = w \cdot x + b$, which corresponds to a separating hyperplane $w \cdot x + b = 0$. Among the separating hyperplanes, the one for which the distance to the closest point is maximal is called the optimal separating hyperplane(OSH). Since the distance to the closest point is $1/\|w\|$, finding the OSH amounts to minimizing $\|w\|^2$ under the constraint. It means that there are two hyperplanes parallel to the classifier hyperplane, which are going to lean against the nearest data in order to center as well as a possible classifier between both classes. The quantity $2/\|w\|$ is called the margin, and it can be seen as a measure of the generalization ability. So it becomes an optimization problem to find the classifier which maximizes the Euclidian distance between both hyperplanes. If we denote by $(\alpha_1,...\alpha_N)$ the N non-negative Lagrange multipliers associated with constraints, our optimization problem amounts to maximizing

$$W(\alpha) = \sum_{i=1}^{N} \alpha_i - \frac{1}{2}\sum_{j=1}^{N} \alpha_i \alpha_j y_i y_j x_i \cdot x_j \tag{3}$$

With $\alpha_i \ge 0$ and under constraint $\sum_{i=1}^{N} y_i \alpha_i = 0$. This can be achieved by the use of standard quadratic programming methods. The solution can be expressed by terms of the linear combination of the training vectors as

$$w = \sum_{i=1}^{N} \alpha_i y_i x_i \tag{4}$$

Only a few a_i will be greater than zero. The corresponding x_i is the support vectors, which lie on the margin and satisfy $|g(x)| = 1$. The classification function can thus be written as

$$f(x) = sign(\sum_{i=1}^{N} \alpha_i y_i x_i \cdot x + b) \tag{5}$$

However, in most cases, we cannot find a linear classifier consistent with the training set: the classification problem is not linearly separable. One solution is to map the input data into a high-dimensional feature space through some nonlinear mapping. In this feature space, the OSH is constructed.

If we replace x it by mapping it in the feature space $\phi(x)$, the dual representation of the optimization problem is then given by the following formula:

$$W(\alpha)=\sum_{i=1}^{N}\alpha_i-\frac{1}{2}\sum_{i=1}^{N}\sum_{j=1}^{N}\alpha_i\alpha_j y_i y_j \phi(x_i)\cdot\phi(x_j) \quad (6)$$

Finding the mapping ϕ is a very difficult problem. Instead of searching for ϕ, it is easier to search directly for a kernel function K defined $K(x_i,x_j)=\phi(x_i)\cdot\phi(x_j)$ to satisfy Mercer's condition. Finally, the decision function becomes

$$f(x)=sign(\sum_{i=1}^{N}\alpha_i y_i K(x_i,x_j)+b) \quad (7)$$

B. Structural Statistical Kernel

The kernel framework is particularly favorable to eddy detection problems because it creates a natural separation between the learning framework and known eddy characteristics that are necessary to craft a meaningful eddy representation. In this study, the mesoscale eddies to detect in sea current images are characterized by currents that flow in a roughly circular motion around the center of the eddy, and they aren't linearly separable. This section describes the construction of a kernel function based on structural statistical information.

Given a sea current image tile, the velocity is represented by a two-dimensional vector (u,v) corresponding to a position in a sea current space. The tile is divided into four parts, and as Figure 1 shows, four values can be obtained by counting the number of times each u is higher than 0 in the four parts. This value demonstrates the distribution of directions in a quarter. Four other values can be obtained by summing up the value of each u in the four parts. This value demonstrates the merging sea current in a quarter, in the same way, eight more values can be determined from v. The computation of the SSF feature is described in formula 8.

$$v_1=\sum_{i=1}^{n^2/4}s(u_i)$$
$$\text{let } s(u_i)=\begin{cases}1 & with\ u_i>0\\ 0 & otherwise\end{cases} \quad (8)$$
$$v_2=\sum_{i=1}^{n^2/4}u_i$$

In this way, the current sea data can be projected into a new structural statistical space E, and the sea current image tile can be represented by a 16-dimensional vector $<v_1,v_2,\cdots,v_{16}>$, as the following figure shows. For that, we introduce the mapping

$$\phi_1:T_s\rightarrow V_s \quad (9)$$

where T_s is a tile data and V_s is a 16-dimensional vector. The graphical representation of this projection is shown in Figure 1.

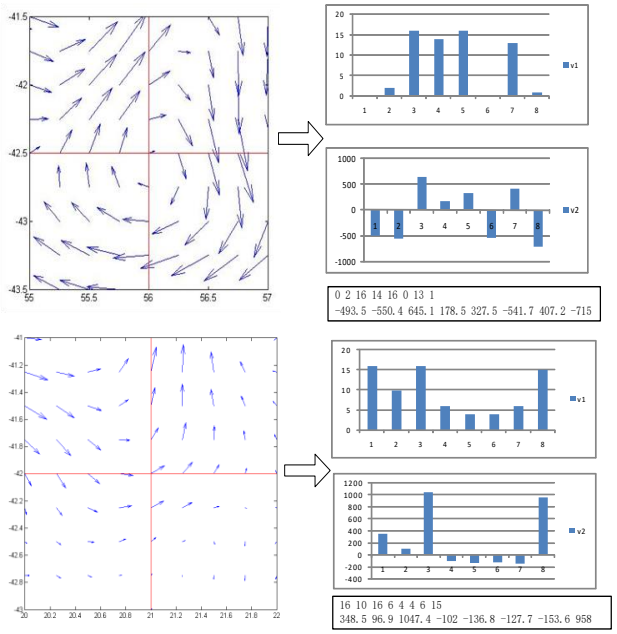

Fig. 1 Examples of SSF extraction, positive case (top) and negative case (bottom)

We compose the final SSF kernel function with a Gaussian kernel K_g in order to obtain a robust kernel. A Gaussian kernel is useful because it enables the calculation of similarity in the space of infinite dimension. Finally, we obtain the following kernel function:

$$\forall(T_s,T_t)\in E \quad (10)$$
$$K(T_s,T_t)=K_g\left(\phi_1(T_s),\phi_1(T_t)\right)=\exp(-\frac{\|V_s-V_t\|^2}{2\sigma^2})$$

Where σ is the variance of the Gaussian kernel? The lower the value of σ, the better the learning of an example. In the experiment, it's set to be 0.05 to avoid the over-learning phenomenon.

C. Processing Workflow

The proposed approach is designed to detect multiple eddies at different locations in an input sea current image. The overall architecture of the eddy detection approach is illustrated in the following figure. One essential component of the proposed approach is an eddy detector, which uses SSF as object representation. In this approach, the eddy detector is formed as a hierarchical classifier that combines histogram matching and a support vector machine.

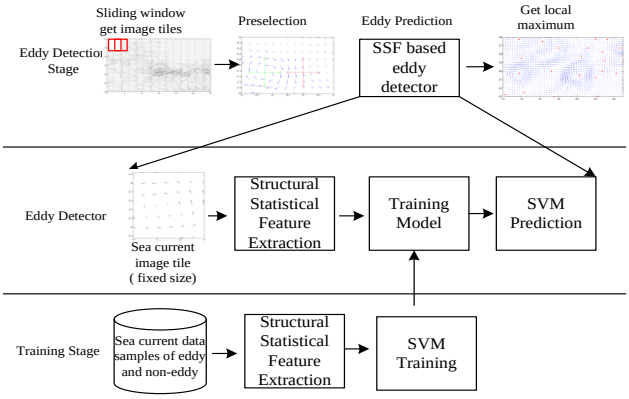

Fig. 2 Workflow of Eddy Detection

Eddy center detection is a two-stage process: A training stage and an eddy detection stage.

The training stage constructs a model of support vectors, which is used later for classification during the eddy detection stage. During the training stage, the SVM is trained using a sample image as input. 16-dimensional structural statistical vectors will be extracted using the mapping algorithm noted above, and the SVM will then be used to train these vectors that, in turn, will generate support vectors as the model output.

During the eddy detection stage, given a shape dataset S of size m, a brute force algorithm is utilized to find the eddies. Each image is traversed to get tiles in the same size as tiles in the training set using the sliding window method. The structural statistical vector of each tile is extracted using the foresaid mapping. We use the SVM to classify whether this tile is eddy with the help of the training model. The detector is applied at every location in the current sea image in order to detect eddies anywhere in the image. The flow chart of this algorithm is shown in Fig. 3.

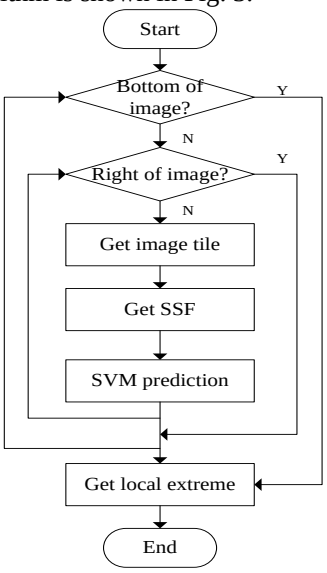

Fig. 3 Flow chart of brute force eddy detection algorithm

IV. EXPERIMENT AND COMPARISON

The algorithm presented here has been applied to current sea data derived from MSLA published by AVISO in a globally uniform 1/4° latitude by 1/4° longitude grid. In the training stage, 895 training tiles (409 positive cases and 486 negative cases) were used, and a model composed of 91 support vectors was generated. Then the model was used to detect eddies from 912 global sea current data.

Comparisons between detected eddy centers and MSLA field, current sea field, and OW parameter were made to test the detection results. This figure shows the eddy centers overlay OW parameter and current sea field. This comparison indicates that the eddies are well detected, and they are in the center of every vortex.

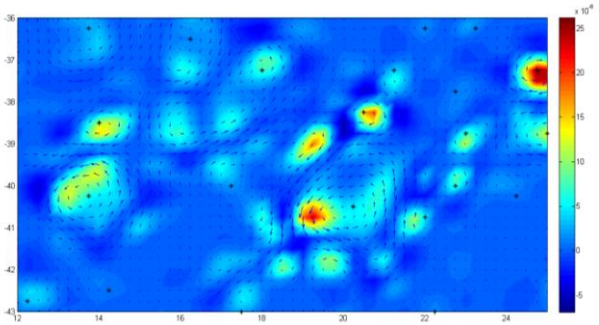

Fig. 4 Sea current and eddy centers, the black '*' presents eddy center

This figure shows the eddy centers overlay MSLA field. It can be seen that every detected eddy center lies at the extremum point in the MSLA field. The MSLA contour-based eddy detection algorithm uses two thresholds(over 0 and below 0) of MSLA to identify an eddy. However, Fig. 6 shows that inside these kinds of detected eddies still lies smaller cyclonic or anticyclonic structures. The SSF based algorithm can recognize these details inside an MSLA contour, and it detects more eddies than the MSLA contour-based eddy detection method.

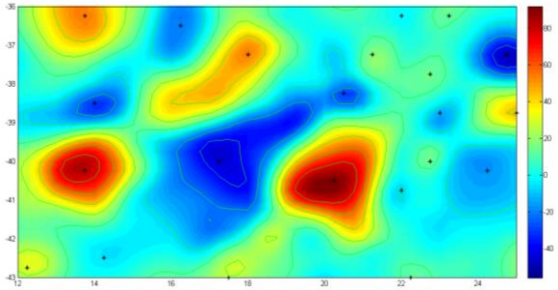

Fig. 5 MSLA and eddy centers, the black '*' presents eddy center

We have also tested our method on a data set of 6374 image tiles, including 1723 eddy cases and 4651 non-eddy cases. The eddy data set is from the result of the OW algorithm, which was visually inspected in the current sea field. The method performs well on both the true and false cases, with a detection accuracy of 97.6%. One potential explanation for the 2.4% false detection rate is that in some cases (see Fig. 8 for examples), the area between two strong

sea currents can form a very long-shaped eddy. When applying the eddy detection algorithm to this area, the SSF extracted from these center tiles is similar to the SSF of the non-eddy area between two strong sea currents. Because of the small differences in SSF, some eddies were detected by mistake, and some real eddies were ignored.

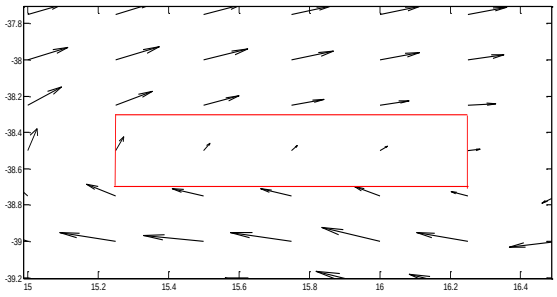

Fig. 6 False case of eddy detection

Fig. 7 shows the distribution of eddy centers for eddies with a lifetime>=4 weeks, and mesoscale eddies can be found nearly everywhere in the world ocean; interestingly, there are some filaments of non-eddy areas that exist in the southern ocean and areas close to Asia and the American continents. Comparison between the top and bottom image shows that only a small part of the mesoscale propagates eastward, and these eastward propagation eddies are concentrated mainly in area 40-60 degrees south latitude.

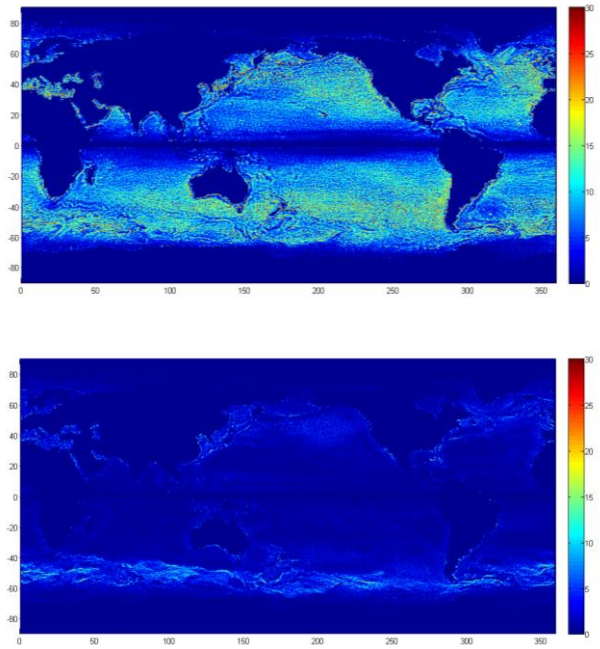

Fig. 7 Statics of eddy centers, for eddies with life time>=4 weeks that passed through each 1/4° by 1/4° region. (Top) all detected eddies, (Bottom) eastward propagation eddies.

V. CONCLUSION AND FUTURE WORK

This study proposed a structural statistical feature-based eddy detection approach. This method is based on statistical learning and kernel function theory; it automatically extracts statistical information from sea current image tiles and learns a hierarchical classifier by combining histogram matching and support vector machine. Experiments show high detection rates with a low number of false detection. These results illustrate the high discriminant power of the SSF based eddy detection approach. As an extension of this work, the SSF based eddy detection method is investigated for sea surface temperature data. The ongoing work includes extracting more eddy properties and using the result data for further statistical analysis and prediction application.

REFERENCES

[1] Robert E. Cheney, Philip L. Richardson, Observed decay of a cyclonic Gulf Stream ring, Deep-Sea Research, and Oceanographic Abstracts, 23(2) (1976) 143-155.

[2] J. Aristegui, P. Tett, A. Hernandez-Guerra, et al., The influence of island-generated eddies on chlorophyll distribution: a study of mesoscale variation around Gran Canaria, Deep-Sea Research Part I: Oceanographic Research Papers, 44(1) (1997) 71-96.

[3] Van Haren, H., C. Millot, and I. Taupier-Letage, Fast deep sinking in Mediterranean eddies, Geophysical Research Letters, L04606, doi:10.1029/2005GL025367, 33(2006).

[4] McWilliams, J. C., The nature and consequence of oceanic eddies. Ocean Modeling in an Eddying Regime, M. W. Hecht and H. H. Hasumi, Eds., AGU, (2008) 5–15.

[5] Renato M. Castelao, Ruoying He, Mesoscale eddies in the South Atlantic Bight. Journal Of Geophysical Research: Oceans, 118 (2013) 5720-5731, doi:10:1002/jgrc.20415.

[6] Vishal Sood, Bin John, Ramprasad Balasubramanian and Amit Tandon, Segmentation and tracking of mesoscale eddies in numeric ocean models. Image Processing, (2005). ICIP 2005.

[7] P.S. Lobel, A.R. Robinson, Transport and entrapment of fish larvae by ocean mesoscale eddies and currents in Hawaiian waters, Deep-Sea Research Part A. Oceanographic Research Papers, 33(4) (1986) 483-500.

[8] Falkowski, Paul G, Ziemann, David, Kolber, Zbigniew, Bienfang, Paul K, Role of eddy pumping in enhancing primary production in the ocean, Nature, Volume 352, Issue 6330, pp. 55-58, July 1991.

[9] D. J. McGillicuddy, Jr, A. R. Robinson, et al. Knap, Influence of mesoscale eddies on new production in the Sargasso Sea, Nature, 394, (6690) (1998) 263-266.

[10] J. D. McNeil, H. W. Jannasch, et al., New chemical, bio-optical and physical observations of the upper ocean response to the passage of a mesoscale eddy off Bermuda, Journal of Geophysical Research, 104(C7) (1999) 15,537-15,548.

[11] Claudia R. Benitez-Nelson et al., Mesoscale Eddies Drive Increased Silica Export in the Subtropical Pacific Ocean, Science 18: 31(2007) 58271017-1021.

[12] Chelton, Dudley B., Schlax, Michael G., Samelson, Roger M., de Szoeke, Roland A, Global observations of large oceanic eddies, Geophysical Research Letters, 34(15) (2007).

[13] Alexis Chaigneau, Arnaud Gizolme, Carmen Grados, Mesoscale eddies off Peru in altimeter records: Identification algorithms and eddy Spatio-temporal patterns, Progress In Oceanography, The northern Humboldt Current System: Ocean Dynamics, Ecosystem Processes, and Fisheries, 79(2-4) (2008) 106-119.

[14] Gary S.E. Lagerloef, Gary T. Mitchum, Roger B. Lukas, Pearn P. Niiler, Tropical Pacific near-surface currents estimated from altimeter, wind, and drifter data, Journal of Geophysical Research, 104(C10) (1999) 23,313-23,326.

[15] Lijuan Qin, Qing Dong, Cunjin Xue, Xueyan Hou, Wanjiao Song, A new method for mesoscale eddy detection based on watershed segmentation algorithm, Proc. SPIE 9261, Ocean Remote Sensing and Monitoring from Space, 92610A; doi: 10.1117/12.2069167, (2014).

[16] Isern-Fontanet, Jordi, Garcia-Ladona, Emilio, Font, Jordi, Identification of marine eddies from altimetric maps, Journal of Atmospheric and Oceanic Technology, 20 (2003) 772-778.

[17] Akira Okubo, Horizontal dispersion of floatable particles in the vicinity of velocity singularities such as convergences, Deep-Sea Research and Oceanographic Abstracts, 17(3) (1970) 445-454.

[18] Francesco Nencioli, Changming Dong, Tommy Dickey, Libe Washburn, James C. McWilliams, A Vector Geometry–Based Eddy Detection Algorithm and Its Application to a High-Resolution Numerical Model Product and High-Frequency Radar Surface Velocities in the Southern California Bight, Journal of Atmospheric and Oceanic Technology 27(3) (2010) 564-579.

[19] V. Vapnik, Statistical Learning Theory, Wiley, NewYork, (1998).

[20] Addis Seid, T. Suryanarayana, "Identification of Lithology and Structures in Serdo, Afar, Ethiopia Using Remote Sensing and Gis Techniques" SSRG International Journal of Geoinformatics and Geological Science 8.1 (2021): 27-41.